X-624-77-122
PREPRINT

TMX-71360

MONTE-CARLO ANALYSIS OF UNCERTAINTY PROPAGATION IN A STRATOSPHERIC MODEL:

I. DEVELOPMENT OF A CONCISE STRATOSPHERIC MODEL

R. D. RUNDEL
D. M. BUTLER
R. S. STOLARSKI

MAY 1977

GSFC — GODDARD SPACE FLIGHT CENTER —
GREENBELT, MARYLAND

X-624-77-122

MONTE-CARLO ANALYSIS OF UNCERTAINTY PROPAGATION IN A STRATOSPHERIC MODEL: I. DEVELOPMENT OF A CONCISE STRATOSPHERIC MODEL

R. D. Rundel
NASA/Johnson Space Center
Houston, TX 77058

D. M. Butler
and
R. S. Stolarski
Laboratory for Planetary Atmospheres
NASA/Goddard Space Flight Center
Greenbelt, Md. 20771

May 1977

MONTE-CARLO ANALYSIS OF UNCERTAINTY PROPAGATION IN A STRATOSPHERIC MODEL: I. DEVELOPMENT OF A CONCISE STRATOSPHERIC MODEL

R. D. Rundel
NASA/Johnson Space Center
Houston, TX 77058

D. M. Butler
and
R. S. Stolarski
Laboratory for Planetary Atmospheres
NASA/Goddard Space Flight Center

ABSTRACT

Analysis of uncertainties in stratospheric perturbations requires the development of a model which uses a minimum of computer time yet is complete enough to reasonably represent the results of more complex models. Such a concise model has been developed and is described in this paper. The model is a steady-state model using iteration to achieve coupling between interacting species. The species N_2O, odd nitrogen, CH_4, CH_3Cl, CCl_4, CF_2Cl_2, $CFCl_3$, and odd chlorine are determined from diffusion equations with appropriate sources and sinks. The HO_x species, O, O^1D and O_3 are solved in photochemical equilibrium and H_2O, H_2, N_2, O_2 and temperature have been assigned fixed profiled. Diurnal effects due to chlorine nitrate formation are accounted for by an analytic approximation. The model has been used to evaluate steady-state perturbations due to injections of chlorine and NO_x. The results are similar to those obtained by other models.

CONTENTS

TABLES

ILLUSTRATIONS

MONTE-CARLO ANALYSIS OF UNCERTAINTY PROPAGATION IN A STRATOSPHERIC MODEL: I. DEVELOPMENT OF A CONCISE STRATOSPHERIC MODEL

INTRODUCTION

In the study of the potential effects of man-made pollutants on the Earth's ozone layer, computer models of the stratosphere have been used extensively to provide quantitative predictions of ozone depletion. These models utilize as inputs experimentally determined transport coefficients, chemical reaction rates, and photodissociation cross-sections, and produce as outputs the concentrations of various chemical species as a function of altitude. In order to make an intelligent assessment of the impact of stratospheric pollution, it is necessary to know not only the predicted ozone depletion, but also the accuracy of this prediction.

There are two kinds of possible inaccuracy in the predictions of ozone depletion from computer models. One kind may arise if the model fails to include some physically significant process, for instance, an important chemical reaction. Possible inaccuracies of this kind cannot be evaluated a priori, but can be identified by careful comparison of model predictions with actual atmospheric measurements.

A second kind of potential inaccuracy, however, is amenable to a priori evaluation. This kind of inaccuracy arises because the model input parameters are experimentally determined quantities, each of which has an uncertainty associated with it. The propagation of these various experimental uncertainties through the model calculation leads to a net uncertainty in the model outputs. In principle, if the distribution of uncertainty can be estimated for each of the input parameters, then standard uncertainty propagation techniques could be used to estimate the uncertainty distribution of the output. In practice, however, the propagation of uncertainties through a model calculation is difficult because of the non-linear feedbacks involved in the radiation absorption in the stratosphere. The magnitude of some of the uncertainties precludes the use of standard error propagation formulas which are derived assuming small errors. A direct way to surmount these difficulties is to use a Monte-Carlo analysis, in which the input variables can be randomly chosen according to their individual probability distributions. The model must then be run enough times to generate a statistically valid distribution in the calculated output. This approach necessitates the development of a model which is fast enough to be run many times without using excess computer resources. At the same time, the model must be sufficiently complete to simulate the complex stratospheric processes not only when the input parameters are at their nominal values, but also when the

input parameters are at their nominal values, but also when they are one or two standard deviations away.

To meet these criteria, a steady-state one-dimensional stratospheric model has been developed using iteration to achieve self-consistency amongst the concentrations of the various species. Liberal use has been made of photochemical equilibrium assumptions. A rather complete chemistry is used for the odd oxygen (O_x), odd nitrogen (NO_x), odd hydrogen (HO_x) and odd chlorine (Cl_x) systems and the radiative feedback processes which work through the dissociation coefficients are included. This paper (paper I) describes the model, while paper II (Stolarski, et. al., 1977) discusses the use of this model for uncertainty analysis.

DESCRIPTION OF MODEL

The model developed for uncertainty studies covers the altitude range from 15 to 50 km in 5 km steps. Because of the use of iteration to achieve self-consistency only single uncoupled diffusion equations are solved. The solutions for 5 km altitude steps have been tested and found to agree with diffusion solutions for 2 km and 1 km steps. The basic chemistry of the odd oxygen, nitrogen, hydrogen, and chlorine compounds is included together with the methane oxidation chain. Fixed profiles are used for the stable molecules N_2, O_2, H_2O, and H_2 and for temperatures (see Table 1). N_2O and CH_4 concentrations are determined from a self-consistent diffusion calculation with fixed lower boundary conditions of 300 ppbv N_2O and 1.5 ppmv CH_4. Except for the species NO, NO_2, ClO and $ClONO_2$, day-night effects are suppressed by diurnal averaging. The method by which these exceptions are treated is given below. Reactions used in the model and their rates, together with estimated uncertainties, are summarized in Table 2.

Photodissociation Coefficients

The calculation of photodissociation coefficients uses the solar flux values reported by Ackerman (1971) as modified by the measurements of Simon (1974). The spectrum is divided into 25 wavelength intervals between 1800 and 3200Å. Dissociation coefficients for the wavelength region beyond 3200Å are calculated assuming no attenuation of the incident solar radiation. The absorption of the incident radiation below 3200Å is assumed to be controlled by O_2 and O_3 while all other species are assumed optically thin. Table 3 shows the cross sections used as a function of wavelength; these values can be readily used along with species concentrations given later in this paper to demonstrate the accuracy of this assumption.

The first two wavelength intervals from 1800 to 2000A contain the Schumann-

Runge absorption bands of O_2. These give rise to a temperature dependent absorption coefficient as described by Hudson and Mahle (1972). Their technique was used to calculate detailed dissociation rates throughout this region for differing O_2 and O_3 column contents as a function of temperature. These were then combined into 100A intervals and best-fit effective cross-sections were obtained as a function of temperature. Because the model extends to only 50 km, this is sufficient detail for all significant processes. A reexamination of these approximations would be necessary to extend the model much beyond 60 km.

The calculated dissociation coefficients were diurnally averaged for the spring-fall season at 30° latitude by the technique described by Rundel (1977). Briefly this consists of recognizing that in a given wavelength interval the ratio, R, of the attenuated solar intensity to the solar intensity at the top of the atmosphere is a function only of the optical depth. This function of optical depth can be diurnally averaged numerically yielding an empirical formula for use in the model. At each altitude and within each wavelength band the optical depths of O_2 and O_3 are calculated and the appropriate diurnally averaged value of R is computed. The dissociation (J) J coefficients for each species and each wavelength are then calculated and the integration over wavelength carried out. This results in considerable time saving over the technique of calculating the wavelength integrated J coefficient and then averaging that quantity over time of day. Figure 1 shows the calculated J coefficients as a function of altitude together with the standard case ozone profile. These values represent 24 hour averages without any effects due to Rayleigh scattering or surface reflection (see e.g. Luther and Gelinas, 1976).

Odd Oxygen

The term "odd oxygen" is customarily used to refer to the sum of the O and O_3 concentrations. Odd oxygen is produced by the photolysis of O_2; it is destroyed by the reaction of O with O_3 and by catalytic cycles involving Cl_X, NO_X, and HO_X. The calculation of destruction rates for the $O+O_3$ reaction and the NO_X and Cl_X cycles is straightforward, but for HO_X it is somewhat complex. For this reason, a generalized concept of odd oxygen has been used and is discussed below in the HO_X section. This concept simplifies the determination of odd oxygen destruction rates. Odd oxygen is essentially in photo-chemical equilibrium above 28 km. Below this altitude, chemical time constants are long compared to transport times and the equilibrium approximation is inappropriate. However, the production and loss rates of odd oxygen have altitude distributions in this region which coincidentally give reasonable ozone distributions. Invoking the photochemical equilibrium assumption results in a large saving in computer time which in turn makes the Monte-Carlo uncertainty analysis feasible.

Figure 2 shows the production and loss rates of odd oxygen due to various reactions. It is interesting to note the differences between this breakdown of odd oxygen loss processes and those calculated 2 or 3 years ago by most modelers. Representative of circa 1974 model results are those of McElroy et al. (1974) which show the odd oxygen loss rate dominated by NO_x reactions between 30 and 40 km by about a factor of 5. Around 45-50 km $O+O_3$ dominates and HO_x reactions don't become dominant until about 55 km. The present results indicate a much larger role for HO_x mainly because of the reduced rate now used for the reaction of OH and HO_2, a rate which is supported by the OH measurements of Anderson (1976). This larger role for HO_x reactions leads to lower calculated ozone concentrations around 50 km. These concentrations are in conflict with existing data such as that summarized by Krueger and Minzner (1976) and more particularly with the recent stellar occultation measurements of Riegler et. al. (1977). This problem has been recognized by a number of modeling groups (see e.g. Frederick (1977), Liu (1977), Sze (1977), Wofsy (1977)).

Odd Nitrogen

The concentration of odd nitrogen (N, NO, NO_2, NO_3, $ClONO_2$, HNO_3) is crucial because the NO-NO_2 catalytic cycle (reactions 14 and 19 in Table 2) is the major ozone destruction mechanism in the natural stratosphere. Odd nitrogen is produced in the stratosphere by the reaction of $O(^1D)$ with N_2O which diffuses upward from the earth's surface and in the mesosphere by the effects of energetic particles or ionizing radiation with subsequent ion-molecule reactions. It is destroyed by diffusion to the troposphere followed by rainout, and by photolysis of NO followed by the reaction of $N(^4S)$ atoms with NO to reform N_2 in the 35 to 65 km region. The available data, shown in figure 3, on total odd nitrogen is sparse but increasing rapidly. Above 45 km, measurements of NO are equivalent to total odd nitrogen, since existing photochemical models, including the present one, predict NO to odd nitrogen ratios greater than .9 in the daytime. Between 35 and 45 km measurements of NO and NO_2 are sufficient to define odd nitrogen. At lower altitudes simultaneous measurements of NO, NO_2, and HNO_3 are required to define the total odd nitrogen concentration. Additionally, at higher latitudes the amount of N_2O_5 may be significant although it has not yet been measured and is not included in this model. As can be seen from figure 3, there is a significant downward flux of odd nitrogen above 60 km from the mesopheric source. The data indicates that by 50 km this flux has reversed sign and odd nitrogen is flowing upward from the stratospheric source to the sink due to photolysis of NO. The upper boundary in the present model is at 50 km, and the bound-condition assumed there is an upward flux of 5×10^7 cm^{-2} sec^{-1} which has been adjusted to obtain a reasonable fit to the data.

Below 50 km, the loss rate of odd nitrogen is calculated by assuming that $N(^4S)$

atoms created by photolysis of NO are in photochemical equilibrium. The loss processes for $N(^4S)$ are reaction with NO (reaction 33) converting two odd nitrogens back to N_2 and reaction with O_2 or O_3 (reactions 34 and 35) reforming NO. Since $N(^4S)$ and NO exist only in the daytime, it is necessary to use daytime averages instead of diurnal averages in calculating the loss rate of odd nitrogen. This has been accomplished in the present model by using the diurnal average results and noting that the NO/NO_2 ratio in the daytime is twice the diurnal average.

Calculation of the dissociation coefficient for NO is extremely difficult because absorption occurs in predissociated bands which overlap the Shumann-Runge bands of O_2. The dissociation rate is thus dependent on the details of the overlap of these two band systems. The most complete study to date is that of Cieslik and Nicolet (1973) and their results at 60° solar zenith angle have been used as representative of the daytime average. In this case, the diurnal averaging technique of Rundel (1977) is not used because it does not apply to non-Beer's law absorption.

The lower boundary condition on odd nitrogen is a fixed mixing ratio at 15 km of 1 ppbv (see Evans, et al., 1976).

Odd Hydrogen

Odd hydrogen (H, OH, HO_2, 2 x H_2O_2, HCl, HNO_3) is produced by reaction of $O^1(D)$ with H_2O (reaction 27), H_2 (reaction 28), and CH_4 (reactions 29 and 30), by reaction of Cl with H_2 (reaction 4) and CH_4 (reaction 6) and by either photolysis of or reaction of O with CH_2O to produce HCO. Although its chemistry is complex, the treatment of odd hydrogen is not computationally difficult in a model because it reacts with itself to reform H_2O rapidly enough to justify the assumption of photochemical equilibrium. The major loss reactions are OH + HO_2 and OH + H_2O_2 (reactions 39 and 40). The chemical lifetime of H_2O_2 in the lower stratosphere (15-20 km) is comparable to the transport time and the photochemical equilibrium assumption is only approximate at that level. In the present model CH is selfconsistently diffused, and the chemistry of its oxidation products is treated in detail. Fixed profiles of H_2O and H_2 assumed.

The major calculational problem involving the odd hydrogen family is the determination of the odd oxygen destruction rate. For odd nitrogen, this is relatively easy because there is only one significant cycle and its rate determining step is readily apparent. For odd hydrogen, however, there is an intricate web of interwoven catalytic destruction cycles. One possible solution is to avoid the use of the concept of a catalytic cycle and count one odd oxygen destroyed for each of the reactions.

$$O + HO_2 \rightarrow OH + O_2$$
$$O_2 + HO_2 \rightarrow OH + 2O_2$$
$$OH + O \rightarrow O_2 + H$$
$$OH + O_3 \rightarrow HO_2 + O_2$$
$$H + O_3 \rightarrow OH + O_2$$

However this neglects a reaction sequence pointed out by Crutzen (1973) which is important in the lower stratosphere and troposphere, namely

$$NO + HO_2 \rightarrow NO_2 + OH$$

followed by

$$NO_2 + h\nu \rightarrow NO + O$$

which produces odd oxygen and reduces the catalytic effect. A simple scheme is presented here to circumvent all such difficulties. The scheme consists of generalizing the concept of odd oxygen to include more species than just O and O_3. When an O_2 molecule is dissociated the O atoms formed may follow many paths. For instance, one may attach to O_2 to form O_3. The O_3 at some point may react with NO, but in this reaction the oxygen atom is simply transferred to NO forming NO_2. Photolysis of NO_2 then returns the oxygen atom to its original form. If, however, reaction occurs between the NO_2 and another oxygen atom the O atom on the NO_2 is recombined with the other O atom for a net loss of two odd oxygens. The identification of the rate determining step of this catalytic cycle naturally follows from considering the extra O atom of NO_2 as an odd oxygen. This scheme is readily generalized by assigning an odd oxygen number to each molecule and then simply balancing each chemical equation to determine if odd oxygen is produced or lost in the reaction. Table 4 shows one reasonable set of odd oxygen number assignments. Note that primarily short-lived radicals are considered odd oxygen and that the total concentration throughout the stratosphere. Column 4 of Table 1 indicates the change in odd oxygen number for each reaction used in the model.

Odd Chlorine

The principle reason for the development of this model is the evaluation of uncertainties in model predictions of chlorine perturbations. To accomplish this, the model is iterated to steady state with an ambient chlorine mixing ratio profile; then, additional chlorine sources are included and the model is iterated to a new steady state. Source calculations for Cl_x are performed by solving the

diffusion equation for each source molecule assuming a fixed mixing ratio at 1 km and zero flux at 50 km. The source molecules originate in the troposphere and are destroyed in the stratosphere by photolysis and for CH_3Cl by reaction with OH. They are assumed to decompose completely at the altitude where they initially react. The Cl_x distribution is calculated by solving the diffusion equation with this source, a lower boundary condition of .1 ppbv and zero flux as an upper boundary condition. For the ambient case, CCl_4 (.1 ppbv) and CH_3Cl (1.0 ppbv) are assumed to be the source molecules yielding an asymptotic Cl_x mixing ratio of 1.5 ppbv. The perturbing source molecules are F-11 and F-12 in the relative amounts indicated by the 1975 release rate data (45% F-11 and 55% F-12; NRC Panel on Atmospheric Chemistry, 1976) and in total amounts varying to give different Cl_x perturbations.

Chemical reactions of Cl, ClO, and HCl, as well as $ClONO_2$ suggested by Rowland et al. (1976), are considered. Day-night effects must be included in detail for an accurate calculation of chlorine nitrate concentration. This is accomplished by (1) assuming that the concentration of HCl does not vary on a 24 hour time scale, (2) approximating the day as twelve hours of constant insolation and twelve hours of darkness, and (3) assuming rapid equilibration of the Cl/ClO ratio. These assumptions permit analytic expressions to be written for the time-dependent day and night $ClONO_2$ concentrations. These expressions are assumed equal at sunrise and sunset and separately averaged over twelve hours. Corresponding ClO day and night average concentrations are obtained, and the daytime value is used for reactions in which the other reactant specie is present only in the daytime (e.g. O or NO). OClO is not considered because its rate of formation by $ClO+O_3$ seems to be too slow to make it an important species (Rundel and Stolarski, 1976). ClOO formation will not significantly effect model results and is not calculated. For a discussion of the implications of the chemistry of OClO and ClOO see Stolarski and Cicerone (1976).

MODEL RESULTS

Ambient Atmosphere

Using the reaction set of Table 2 and the boundary conditions and approximations described above, the model was iterated until steady-state was achieved. Figure 4 shows the resulting mixing ratio profiles for CH_4, N_2O, and CO, and the assumed profiles for H_2 and H_2O. The eddy coefficient used was two times that of Hunten (see Johnston, et al., 1976), rising exponentially from 4×10^3 at 15 km to 2×10^5 at 50 km. The resulting mixing ratio of CH_4 at 50 km is 200 ppbv, in reasonable agreement with the measurements of Ehhalt, et al. (1972, 1974). The calculated N_2O profile is in the range of the mid-latitude results of Schmeltekpof, et. al., (1977).

Figure 5 shows the calculated number densities of the HO_x constituents H, OH, HO_2, and H_2O_2 plus those of O and $O(^1D)$. Figure 6 shows the densities of odd nitrogen constituents, NO, NO_2 and HNO_3 together with the total odd nitrogen mixing ratio. Figure 7 shows the HCl, ClO and Cl when the Cl_x asymptotic mixing ratio is 1.5 ppbv. The odd chlorine mixing ratio profile is also shown.

Effects of Chlorine Perturbations

Calculations of the stratospheric Cl_x profile indicate only minor differences in the profile shape for different sources (see e.g. Cicerone et al., 1975). This profile begins just above the tropopause with a very low value of .1 ppbv, increases rapidly and then levels off to a constant asymptotic mixing ratio. Measurements of HCl by Lazurus, et al. (1975), Williams et al. (1976), Farmer et al., (1976), Ackerman et al. (1976) and Eyre and Roscoe (1977) tend to confirm this shape. One of the profiles of Lazrus (1977) shows a falloff at high altitudes larger than can be explained by conversion to ClO. Additionally the concentration of ClO measured by Anderson et al. (1977) is larger than would be expected either from known sources or from the measured HCl concentration. These measurements are thus inconclusive so until more frequent and simultaneous observations of all chlorine species are made, it seems reasonable to assume the shape described above to be correct. Accordingly, runs of the model were made with an ambient Cl_x profile, and then with varying amounts of chlorine added. The mechanism for this was always an F-11 and F-12 addition at the lower boundary of the source calculation in the ratio 45% to 55%. The change in the ozone content due to the addition of chlorine, is shown in Figure 8 as a function of the asymptotic ClX mising ratio for a standard case and for models where the assumed H_2O profile or the N_2O lower boundary condition was varied by a factor of 2. Although these results were generated for F-11 and F-12 they should be relatively independent of the source. The slope of the curve in figure 8 can be interpreted as the ozone destruction efficiency. This concept has been previously used effectively by Wofsy and McElroy (1974) and Donahue et al. (1976). The results for large chlorine perturbations are shown as a model diagnostic. Any results with more than about 10% ozone depletion should be viewed with skepticism because of the possibility of a breakdown of model assumptions.

Effects of NO_x Perturbations

The model was also run with an additional injection of NO_x at 20 km to simulate the potential effect of an SST fleet. Because of the altitude step size, the injection is in a 5 km wide band around 20 km. Figure 9 shows the results for the same five cases. The curve crossings at low NO_x injection are caused by $ClONO_2$ formation decreasing the catalytic efficiency of the ambient Cl_x.

SUMMARY AND CONCLUSION

This paper has described a one-dimensional, steady-state, diurnally-averaged model of stratospheric photochemistry specifically designed to address the question of the propagation of reaction rate uncertainties and the implications on the resultant precision of model results. This model has been shown, despite its simplicity and calculational speed, to adequately reproduce the effects calculated using significantly more complex models. Thus an uncertainty propagation analysis performed on this model should simulate reasonably well the results which would be obtained by such an analysis on a more complex model. The analysis will probably never be carried out on a "complete" model because of computer time limitations.

Acknowledgements

We gratefully acknowledge useful discussions with Robert D. Hudson, Robert T. Watson and Ralph J. Cicerone. We thank Donald J. Kessler who determined the temperature dependent curve fits for the Schumann-Runge Bands. One of us (DMB) wishes to thank the National Academy of Sciences for a Resident Research Associateship at Goddard Space Flight Center during which most of this work was carried out.

REFERENCES

1. Ackerman, M., "Ultraviolet solar radiation related to mesospheric processes" in Mesospheric Models and Related Experiments ed. by G. Fiocco, D. Reidel, publ, Dordrecht, Holland p. 149- (1971).

2. Ackerman, M., J. -C., Fontanella D. Frimout, and A. Girard, "Simultaneous measurements of NO and NO_2 in the stratosphere", Planet. Space Sci., 23, 651-660, (1975).

3. Ackerman, M., D. Frimout, A. Girard, M. Gottignies and C. Muller "Stratospheric NCl from Infrared Spectra", Geophys. Res. Lett., 3, 81 (1976).

4. Anderson, J. G., J. J. Margitorn and D. H. Stedman, "Free Chlorine in the Stratosphere: An IN SITU Study of Cl and ClO", unpublished manuscript, February, 1977.

5. Cicerone, R. J., D. H. Stedman and R. S. Stolarski, "Estimate of late 1974 stratospheric concentration of gaseous chlorine compounds (ClX)", Geophys. Res. Lett., 2, 219 (1975).

6. Crutzen, P., "A discussion of the chemistry of some minor constituents in the stratosphere and troposphere", PAGEOPH 106-108, 1385-1399 (1973).

7. Donahue, T. M., R. J. Cicerone, S. C. Liu, and W. L. Chameides, "Effect of add hydrogen on ozone depletion by chlorine reactions", Geophys. Res. Lett., 3, 105-108, 1976.

8. Drummond, J. W., J. M. Rosen, D. J. Hofmann, "Balloon-borne chemiluminescent measurement of NO to 45 km", Nature, 265, 319 (1977).

9. Ehhalt, D. H., L. E. Heidt, and E. A. Martell, "The concentration of methane between 44 and 62 kilometers altitude", J. Geophys. Res., 77, 2193- (1972).

10. Ehhalt, D. H., L. E. Heidt, R. H. Lueb, and N. Roper, "Vertical profiles of CH_4, H_2, CO N_2O and CO_2 in the stratosphere", Proc. Third Conference on CIAP, ed. by A. J. Broderick and T. M. Hard. DOT-TSC-OST-74-15, pg. 153-160 (1974).

11. Evans, W. F., J. B. Kerr, and D. I. Wardle, "The AES stratospheric

ballon measurements project: preliminary results", Proc. Fourth Conference on CIAP, ed., by T. M. Hard and A. J. Broderic, DOT-TSC-OST-75-38, pg. 412-416 (1976).

12. Eyre, J. R. and H. K. Roscoe, "Radiometric measurement of stratospheric HO", Nature, 266, 243-244 (1977).

13. Framer, C. B., O. F. Raper and R. H. Norton, "Stectroscopic detection and vertical distribution of HCl in the troposphere and stratosphere", Geophys. Res. Lett., 3, 13 (1976).

14. Frederick, J. E., P. B. Hays and S. C. Liu, "The need for a revised theory of mesospheric ozine", EOS, in press (1977).

15. Horvath, J. J. and C. J. Mason, personal communication (1976).

16. Hudson, R. D. and S. H. Mahle, "Photodissociation rates of molecular oxygen in the mesosphere and lower thermosphere", J. Geophys. Res., 77, 2902 (1972).

17. Johnston, H. S., D. Kattenhorn and G. Whitten, "Use of excess carbon 14 data to calibrate models of stratospheric ozone depletion by supersonic transports", J. Geophys. Res., 81, 368-380 (1976).

18. Krueger, A. J., and R. A. Minzner, "A mid-latitude ozone model for the 1976 U.S. standard atmosphere", J. Geophys. Res., 81, 4477 (1976).

19. Liu, S. C. and R. J. Cicerone, "Comparison of theory and measurement of ozone above 35 km", EOS in press, 1977.

20. Lazrus, Al L., B. W. Gandrud, R. N. Woodard, and W. A. Sedlacek, "Stratospheric Halogen Measurements", Geophys. Res. Lett., 2, 439 (1975).

21. Lazrus, A., Position paper on Hydrogen Halide Compounds in the Stratosphere presented at NASA CFM assessment workshop, Warrenton, Va., Jan. (1977).

22. Luther, F. M. and R. J. Gelinas, "Effect of molecular multiple scattering and surface albedo on atmospheric photodissociation rates", J. Geophys. Res., 81, 1125-1132 (1976).

23. McElroy, M. B., S. C. Wofsy, J. E. Penner and J. C. McConnell,

"Atmospheric Ozone: Possible Impact of Stratospheric Aviation", J. Atmos Sci., 81, 287-303 (1974).

24. Meira, L., "Rocket measurements of upper atmosphere nitric oxide and their consequences to the lower ionosphere", J. Geophys. Res., 76, 202 (1971).

25. National Research Council Panel on Atmospheric Chemistry., Halocarbons: Effects on Stratospheric Ozone, Washington, D.C., September, 1976.

26. Riegler, G. R., S. K. Atreya, T. M. Donahue, S. C. Liu, B. Wasser and J. F. Orake, "UV Stellar Occultation Measurements of Nighttime Equatorial Ozone", Geophys. Res. Lett., in press (1977).

27. Rowland, F. S., J. E. Spencer, and M. J. Molina, "Stratospheric Formation and Photolysis of Chlorine Nitrate", J. Phys. Chem., 80, 2711-2713 (1976).

28. Rundel, R. D. and R. S. Stolarski, "A reexamination of the photochemistry of the Cl_2 - O_3 system", J. Geophys. Res., 81, 5759-5764 (1976).

29. Rundel, R. D., "Determination of diurnal average photodissociation rates", J. Atmos. Sci., (1977), in press.

30. Schmeltekopf, A. L., D. L. Albritton, P. J. Crutzen, P. D. Goldan, W. J. Harrop, W. R. Henderson, J. R. McAfee, M. McFarland, H. I. Schiff, T. L. Thompson, D. J. Hofmann and N. T. Kjome, "Stratospheric Nitrous Oxide Altitude Profiles at Various Latitudes", Position paper presented at NASA CFM assessment workshop, Warrenton, VA, January (1977).

31. Simon, P., "Balloon measurements of solar fluxes between 1960 Å and 2300 Å", in Proc. Third Conference on CIAP, ed. by A. J. Broderick and T. M. Hard, DOT-TSC-OST-74-15, O. 137-142 (1974).

32. Stolarski, R. S. and R. J. Cicerone, "Chlorine in the stratosphere", Proc. Fourth Conference on CIAP, ed. by T. M. Hard and A. J. Broderick DOT-TSC-OST-75-38, pg. 280-285 (1976).

33. Stolarski, R. S., D. M. Butler and R. D. Rundel, "Monte-Carlo analysis of uncertainty propagation in a stratospheric model: II. Application to reaction rate uncertainties", submitted to J. Geophys. Res. (1977).

34. Sze, N. D., "Atmosphere ozone: Comparison of theory and observations", EOS, in press (1977).

35. Tisone, G., "Measurements of NO densities during sunrise at Kauai", J. Geophys. Res., [illegible], 746- (1973).

36. Wofsy, S. C. and M. B. McElroy, "HO_X, NO_X and ClO_X: their role in atmospheric photoshemistry", Can. J. Chem., 52, 1582 (1974).

37. Wofsy, S. C., "Temporal and latitudinal variations of stratospheric trace gases: A critical comparison between theory and experiment", submitted to J. Geophys. Res. (1977).

Table 1

Fixed Input Profiles

Altitude (km)	N_2 (cm^{-3})	O_2 (cm^{-3})	H_2O (cm^{-3})	H_2 (cm^{-3})	T (°K)
15	3.20(18)	8.49(17)	1.28(13)	1.99(12)	215
20	1.46(18)	3.87(17)	6.81(12)	8.70(11)	216
25	6.60(17)	1.75(17)	3.53(12)	3.69(11)	221
30	3.03(17)	8.02(16)	1.84(12)	1.59(11)	226
35	1.39(17)	3.69(16)	9.31(11)	7.12(10)	236
40	3.24(16)	8.59(15)	2.34(11)	2.32(10)	264
50	1.69(16)	4.48(15)	1.18(11)	1.78(10)	271

Table 2

Reaction Rates and Uncertainties

	REACTION	RATE ($cm^3\ sec^{-1}$ or $cm^6 sec^{-1}$)	UNCERTAINTY (1σ in log k)	ΔOdd Oxygen
1.	$Cl+O_3 \rightarrow ClO+O_2$	$2.7 \cdot 10^{-11}\ e^{-257/T}$	.06	0
2.	$ClO+O \rightarrow Cl+O_2$	$7.7 \cdot 10^{-11}\ e^{-130/T}$	.06	-2
3.	$ClO+NO \rightarrow Cl+NO_2$	$2.2 \cdot 10^{-11}$	.15	0
4.	$Cl+H_2 \rightarrow HCl+H$	$3.5 \cdot 10^{-11}\ e^{-2290/T}$	.04	0
5.	$Cl+HO_2 \rightarrow HCl+O_2$	$3.0 \cdot 10^{-11}$	.30	0
6.	$Cl+CH_4 \rightarrow HCl+CH_3$	$7.3 \cdot 10^{-12}\ e^{-1260/T}$	(+).06 (-).18	0
7.	$CL+H_2O_2 \rightarrow HCl+HO_2$	$1.7 \cdot 10^{-12}\ e^{-384/T}$	.18	0
8.	$HCl+OH \rightarrow Cl+H_2O$	$3.0 \cdot 10^{-12}\ e^{-425/T}$	.05	-1
9.	$ClO+NO_2+M \rightarrow ClONO_2+M$	$5.1 \cdot 10^{-33}\ e^{+1030/T}$	(+).06 (-).15	0
10.	$ClONO_2+O \rightarrow ClO+NO_3$	$4.5 \cdot 10^{-12}\ e^{-840/T}$	.30	0
11.	$ClONO_2+OH \rightarrow$ products	$1.2 \cdot 10^{-12}\ e^{-333/T}$	.18	0
12.	$O+O_2+M \rightarrow O_3+M$	$1.07 \cdot 10^{-34}\ e^{+510/T}$	.07	0
13.	$O+O_3 \rightarrow O_2+O_2$	$1.9 \cdot 10^{-11}\ e^{-2300/T}$	.10	-2
14.	$NO+O_3 \rightarrow NO_2+O_2$	$2.1 \cdot 10^{-12}\ e^{-1450/T}$	.08	0
15.	$NO_2+O_3 \rightarrow NO_3+O_2$	$1.2 \cdot 10^{-13}\ e^{-2450/T}$	.04	0
16.	$OH+O_3 \rightarrow HO_2+O_2$	$1.5 \cdot 10^{-12}\ e^{-1000/T}$	.15	-2
17.	$HO_2+O_3 \rightarrow OH+O_2+O_2$	$1.0 \cdot 10^{-13}\ e^{-1525/T}$	.30	0
18.	$H+O_3 \rightarrow OH+O_2$	$1.2 \cdot 10^{-10}\ e^{-560/T}$	.15	0
19.	$NO_2+O \rightarrow NO+O_2$	$9.1 \cdot 10^{-12}$	.03	-2
20.	$NO_2+O+M \rightarrow NO_3+M$	$1.0 \cdot 10^{-31}$	.20	0
21.	$OH+O \rightarrow H+O_2$	$1.0 \cdot 10^{-10}\ e^{-250/T}$	.15	-2
22.	$HO_2+O \rightarrow OH+O_2$	$1.0 \cdot 10^{-10}\ e^{-250/T}$	.15	0
23.	$H_2O_2+O \rightarrow OH+HO_2$	$2.75 \cdot 10^{-12}\ e^{-2125/T}$	.15	0
24.	$HNO_3+O \rightarrow OH+NO_3$	$1.0 \cdot 10^{-14}$	(+).15 (·).1.0	0
25.	$CH_2O+O \rightarrow HCO+OH$	$2.0 \cdot 10^{-11}\ e^{-1450/T}$	.20	0
26.	$N_2O+O(^1D) \rightarrow NO+NO$	$5.5 \cdot 10^{-11}$	.10	+1

Table 2 Reaction Rates and Uncertainties (Continued)

	REACTION	RATE (cm^3sec^{-1} or cm^6 sec^{-1})	UNCERTAINTY (1σ in log k)	Δ Odd Oxygen
27.	$H_2O+O(^1D)\rightarrow OH+OH$	$2.3\cdot10^{-10}$	.05	+1
28.	$H_2+O(^1D)\rightarrow OH+H$	$9.9\cdot10^{-11}$	.05	0
29.	$CH_4+O(^1D)\rightarrow OH+CH_3$	$1.3\cdot10^{-10}$	.05	0
30.	$CH_4+O(^1D)\rightarrow H_2+CH_2O$	$1.4\cdot10^{-11}$	.10	0
31.	$O(^1D)+M\rightarrow O(^3P)+M$	$2.0\cdot10^{-11}$ $e^{+107/T}$	.05	0
32.	$NO+NO_3\rightarrow NO_2+NO_2$	$8.7\cdot10^{-12}$	.70	0
33.	$N+NO\rightarrow N_2+O$	$8.2\cdot10^{-11}$ $e^{-410/T}$	.10	0
34.	$N+O_2\rightarrow NO+O$	$5.5\cdot10^{-12}$ $e^{-3220/T}$	.10	+2
35.	$N+O_3\rightarrow NO+O_2$	$5.0\cdot10^{-12}$ $e^{-650/T}$	.30	0
36.	$NO+HO_2\rightarrow NO_2+OH$	$1.5\cdot10^{-11}$ $e^{-1100/T}$	.20	+2
37.	$NO_2+OH+M\rightarrow HNO_3+M$	(see expression below)	.05	0
38.	$OH+HNO_3\rightarrow NO_3+H_2O$	$8.0\cdot10^{-14}$	.05	-1
39.	$OH+H_2O_2\rightarrow HO_2+H_2O$	$1.0\cdot10^{-11}$ $e^{-750/T}$	.15	-1
40.	$OH+HO_2\rightarrow O_2+H_2O$	$3.0\cdot10^{-11}$	.25	-1
41.	$OH+OH\rightarrow O+H_2O$	$1.0\cdot10^{-11}$ $e^{-550/T}$	.20	-1
42.	$OH+H_2\rightarrow H+H_2O$	$8.0\cdot10^{-12}$ $e^{-2100/T}$	.10	-1
43.	$OH+CH_4\rightarrow CH_3+H_2O$	$2.36\cdot10^{-12}$ $e^{-1710/T}$	.10	-1
44.	$OH+CH_2O\rightarrow HCO+H_2O$	$3.0\cdot10^{-11}$ $e^{-250/T}$	.20	-1
45.	$OH+CH_3Cl\rightarrow CH_2Cl+H_2O$	$2.2\cdot10^{-12}$ $e^{-1142/T}$	.10	-1
46.	$OH+CO\rightarrow CO_2+H$	$1.4\cdot10^{-13}$	.10	-2
47.	$OH+OH+M\rightarrow H_2O_2+M$	$1.25\cdot10^{-32}$ $e^{+900/T}$	.15	-2
48.	$H+O_2+M\rightarrow HO_2+M$	$2.1\cdot10^{-32}$ $e^{+290/T}$	.10	0
49.	$HO_2+HO_2\rightarrow H_2O_2+O_2$	$5.0\cdot10^{-12}$ $e^{-500/T}$	.30	0
50.	$CH_3+O_2+M\rightarrow CH_3O_2+M$	$3.85\cdot10^{-31}$	.50	+2
51.	$CH_3O_2+NO\rightarrow CH_3O+NO_2$	$3.3\cdot10^{-12}$ $e^{-500/T}$	1.0	0
52.	$CH_3O_2+NO_2\rightarrow CH_3O+NO_3$	$1.0\cdot10^{-13}$	1.0	0
53.	$CH_3O_2+HO_2\rightarrow CH_3OOH+O_2$	$6.7\cdot10^{-14}$	1.0	0
54.	$CH_3O+O_2\rightarrow CH_2O+HO_2$	$1.6\cdot10^{-13}$ $e^{-3300/T}$	1.0	0
55.	$HCO+O_2\rightarrow CO+HO_2$	$6.0\cdot10^{-12}$	.20	0

Table 2 Reaction Rates and Uncertainties (Continued)

for HNO_3 formation the following expression was employed:

$\log_{10} k = -AT/(B+T)$

where: $A = -10.4432 + 6.33Z - .432126Z^2 + 8.47677 \cdot 10^{-3}Z^3$

$B = 327.372 + 44.5586Z - 1.38092Z^2$

$Z = \log_{10} [M]$

Table 3: Solar Flux and Crossections

Solar flux is in photons/cm^2 sec; Crossection are in cm^2; Visible J-Coefficient are in sec^{-1}.

λλ (Å)	Solar Flux	O_2	O_3	HNO_3	H_2O_2	N_2O	$ClONO_2$	HCl	CH_2O →	CH_2O → HCO	CCl_4	CH_3Cl	$CFCl_3$	CF_2Cl_2
1800 – 1900	1.7 (12)	a	6.0 (-19)	1.8 (-17)	1.1 (-18)	1.1 (-19)	1.0 (-17)	3.1 (-19)	0.0	0.0	7.2 (-18)	6.4 (-19)	3.2 (-18)	1.8 (-18)
1900 – 2000	4.6 (12)	a	3.4 (-19)	9.1 (-18)	6.0 (-19)	5.6 (-20)	5.1 (-18)	6.2 (-20)	0.0	0.0	1.3 (-18)	1.3 (-19)	1.8 (-18)	5.9 (-19)
2000 – 2050	4.0 (12)	1.2 (-23)	3.1 (-19)	3.7 (-18)	4.9 (-19)	2.3 (-20)	3.6 (-18)	1.6 (-20)	0.0	0.0	6.6 (-19)	1.7 (-20)	6.6 (-19)	8.7 (-20)
2050 – 2100	7.5 (12)	1.0 (-23)	3.4 (-19)	1.6 (-18)	4.1 (-19)	1.3 (-20)	3.5 (-18)	6.2 (-21)	0.0	0.0	5.9 (-19)	5.9 (-21)	3.3 (-19)	2.5 (-20)
2100 – 2150	2.1 (13)	7.8 (-24)	7.0 (-19)	5.4 (-19)	3.5 (-19)	5.0 (-21)	3.6 (-18)	2.3 (21)	0.0	0.0	4.7 (-19)	1.9 (-21)	1.5 (-19)	7.8 (-21)
2150 – 2200	2.4 (13)	6.0 (-24)	1.2 (-18)	2.2 (-19)	3.2 (-19)	2.0 (-21)	3.8 (-18)	8.1 (-22)	0.0	0.0	3.0 (-19)	6.5 (-22)	6.1 (-20)	2.1 (-21)
2200 – 2250	3.1 (13)	4.3 (-24)	2.1 (-18)	1.1 (-19)	2.6 (-19)	8.0 (-22)	3.4 (-18)	2.2 (-22)	0.0	0.0	1.7 (-19)	2.3 (-22)	2.4 (-20)	0.0
2250 – 2300	3.4 (13)	3.0 (-24)	3.3 (-18)	6.9 (-20)	2.2 (-19)	3.0 (-22)	2.7 (-18)	0.0	0.0	0.0	8.6 (-20)	0.0	8.8 (-21)	0.0
2300 – 2350	3.6 (13)	1.7 (-24)	5.3 (-18)	4.6 (-20)	1.8 (-19)	7.0 (-23)	1.9 (-18)	0.0	0.0	0.0	4.1 (-20)	0.0	0.0	0.0
2350 – 2400	3.6 (13)	9.0 (-25)	7.0 (-18)	3.1 (-20)	1.4 (-19)	1.4 (-23)	1.4 (-18)	0.0	0.0	0.0	1.9 (-20)	0.0	0.0	0.0
2400 – 2450	4.5 (13)	4.0 (-25)	9.0 (-18)	2.3 (-20)	1.0 (-19)	5.0 (-24)	1.0 (-18)	0.0	0.0	0.0	0.0	0.0	0.0	0.0
2450 – 2500	4.7 (13)	0.0	1.1 (-17)	2.0 (-20)	7.0 (-20)	2.0 (-24)	7.5 (-19)	0.0	0.0	0.0	0.0	0.0	0.0	0.0
2500 – 2550	5.5 (13)	0.0	1.1 (-17)	1.9 (-20)	5.0 (-20)	1.0 (-24)	5.8 (-19)	0.0	0.0	0.0	0.0	0.0	0.0	0.0
2550 – 2600	6.0 (13)	0.0	1.1 (-17)	1.9 (-20)	3.4 (-20)	0.0	4.6 (-19)	0.0	0.0	0.0	0.0	0.0	0.0	0.0
2600 – 2650	8.3 (13)	0.0	1.0 (-17)	1.9 (-20)	2.0 (-20)	0.0	3.7 (-19)	0.0	0.0	0.0	0.0	0.0	0.0	0.0
2650 – 2700	1.7 (14)	0.0	8.6 (-18)	1.7 (-20)	1.0 (-20)	0.0	2.9 (-19)	0.0	0.0	0.0	0.0	0.0	0.0	0.0
2700 – 2750	1.6 (14)	0.0	6.5 (-18)	1.5 (-20)	5.0 (-21)	0.0	2.3 (-19)	0.0	0.0	0.0	0.0	0.0	0.0	0.0
2750 – 2800	1.7 (14)	0.0	4.6 (-19)	1.3 (-20)	1.0 (-22)	0.0	1.7 (-19)	0.0	0.0	0.0	0.0	0.0	0.0	0.0
2800 – 2850	2.1 (14)	0.0	3.0 (-18)	1.0 (-20)	0.0	0.0	1.2 (-19)	0.0	0.0	0.0	0.0	0.0	0.0	0.0
2850 – 2900	2.9 (14)	0.0	1.8 (-18)	7.5 (-21)	0.0	0.0	8.8 (-20)	0.0	0.0	0.0	0.0	0.0	0.0	0.0
2900 – 2950	4.6 (14)	0.0	1.0 (-18)	5.2 (-21)	0.0	0.0	6.1 (-20)	0.0	0.0	0.0	0.0	0.0	0.0	0.0
2950 – 3000	4.5 (14)	0.0	5.2 (-19)	3.4 (-21)	0.0	0.0	4.5 (-20)	0.0	0.0	0.0	0.0	0.0	0.0	0.0
3000 – 3050	4.6 (14)	0.0	2.7 (-19)	2.2 (-21)	0.0	0.0	3.3 (-20)	0.0	2.6 (-21)	7.2 (-22)	0.0	0.0	0.0	0.0
3050 – 3100	5.8 (14)	0.0	1.4 (-19)	1.3 (-21)	0.0	0.0	2.4 (-20)	0.0	2.1 (-21)	1.1 (-21)	0.0	0.0	0.0	0.0
3100 – 3200	1.2 (15)	0.0	5.5 (-20)	4.7 (-22)	0.0	0.0	1.5 (-20)	0.0	1.6 (-21)	1.5 (-21)	0.0	0.0	0.0	0.0
Visible J-Coefficient		0.0	3.76 (-4)	5.23 (-8)	6.87 (-6)	0.0	6.16 (-5)	0.0	3.67 (-8)	1.06 (-5)	0.0	0.0	0.0	0.0

a – For O_2 in the 1800 – 2000 Å interval we use the method described in the text to treat the Schumann-Runge bands.

Table 4

	Odd Oxygen	Odd Nitrogen	Odd Hydrogen	Odd Chlorine
O_3	1	0	0	0
O	1	0	0	0
N	0	1	0	0
NO	1	1	0	0
NO_2	2	1	0	0
NO_3	3	1	0	0
HNO_3	3	1	1	0
H	0	0	1	0
OH	1	0	1	0
HO_2	0	0	1	0
H_2O_2	1	0	0	0
CO	1	0	0	0
CH_3	0	0	1	0
CH_3O_2	2	0	1	0
CH_3O	1	0	1	0
H_2CO	1	0	0	0
HCO	1	0	1	0
CH_3OOH	2	0	2	0
Cl	0	0	0	1
HCl	0	0	1	1
ClO	1	0	0	1
N_2O_5	5	2	0	0
$ClONO_2$	3	1	0	1

The following species in the model have only zero odd species numbers:

O_2, N_2, CO_2, CH_4, N_2O, H_2O, H_2

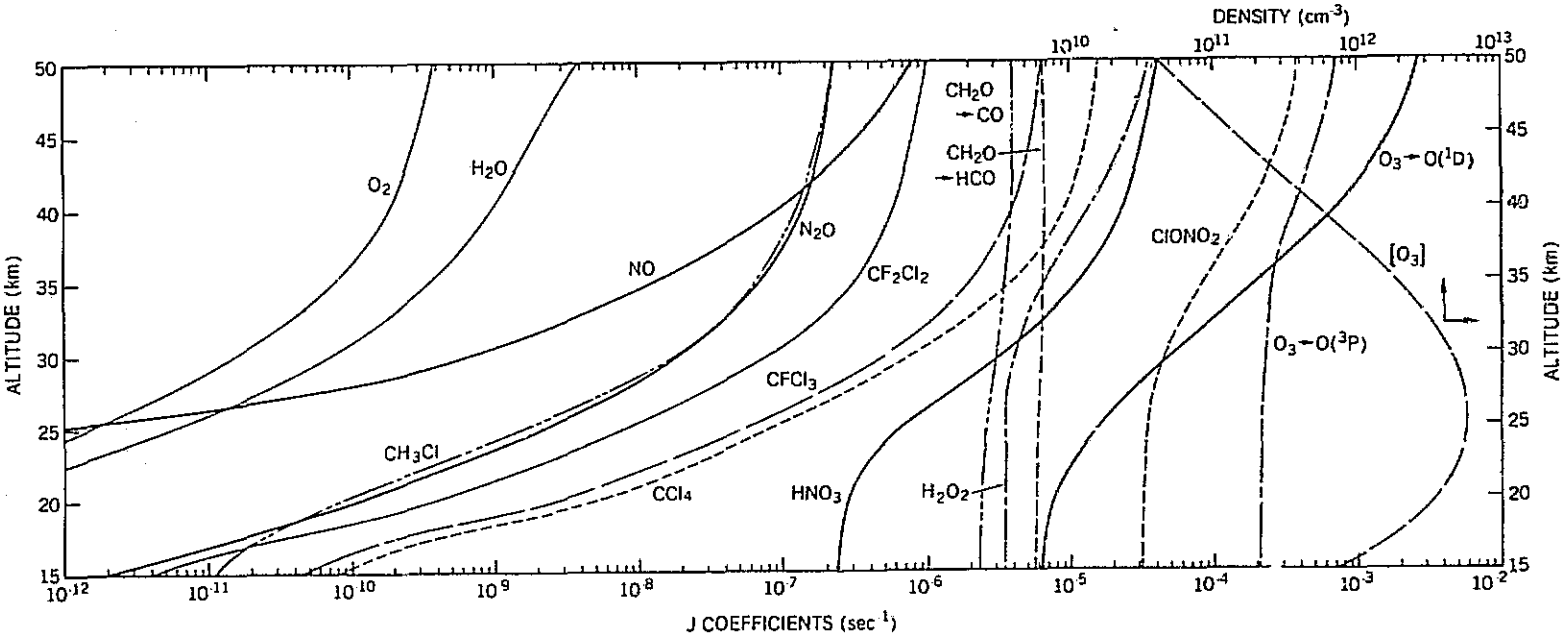

Figure 1. Calculated 24 hour diurnal average J coefficients as a function of altitude. The standard case ozone profile used in the calculations is also given in figure. For $h\nu + NO_2 \rightarrow NO + O$, $h\nu + NO_3 \rightarrow NO_2 + O$, and $h\nu + NO_3 \rightarrow NO + O_2$ constant J-coefficients were used. The values were .005, .05, and .02 sec^{-1} respectively. The dissociation of NO is discussed in the text.

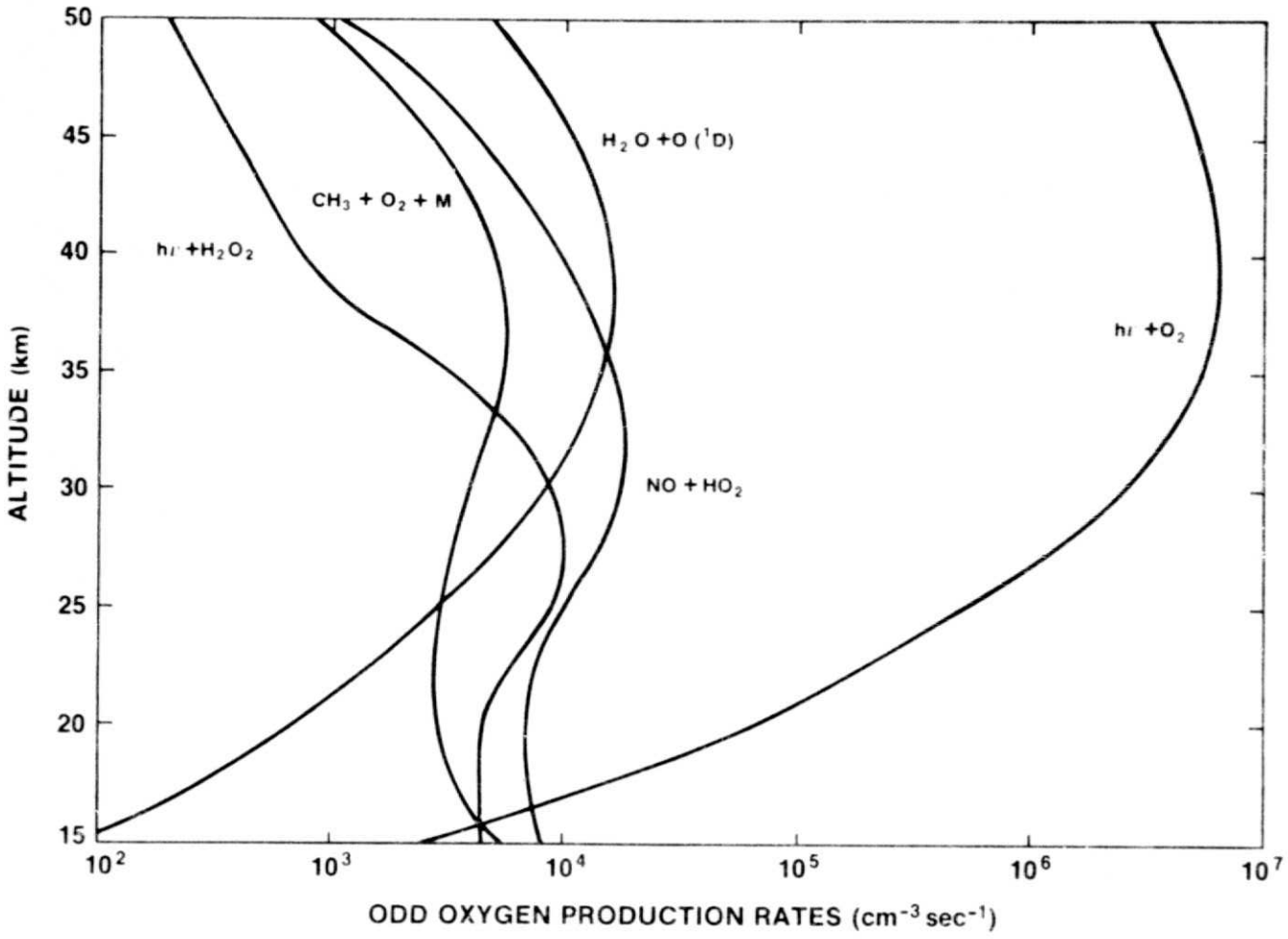

Figure 2a. Production rates (a) and loss frequencies (b) of odd oxygen due to various processes as a function of altitude for $Cl_X = 1.5$ ppbv. Loss frequency is defined as the volume loss rate in $cm^{-3}\,sec^{-1}$ divided by the odd oxygen concentration in cm^{-3}.

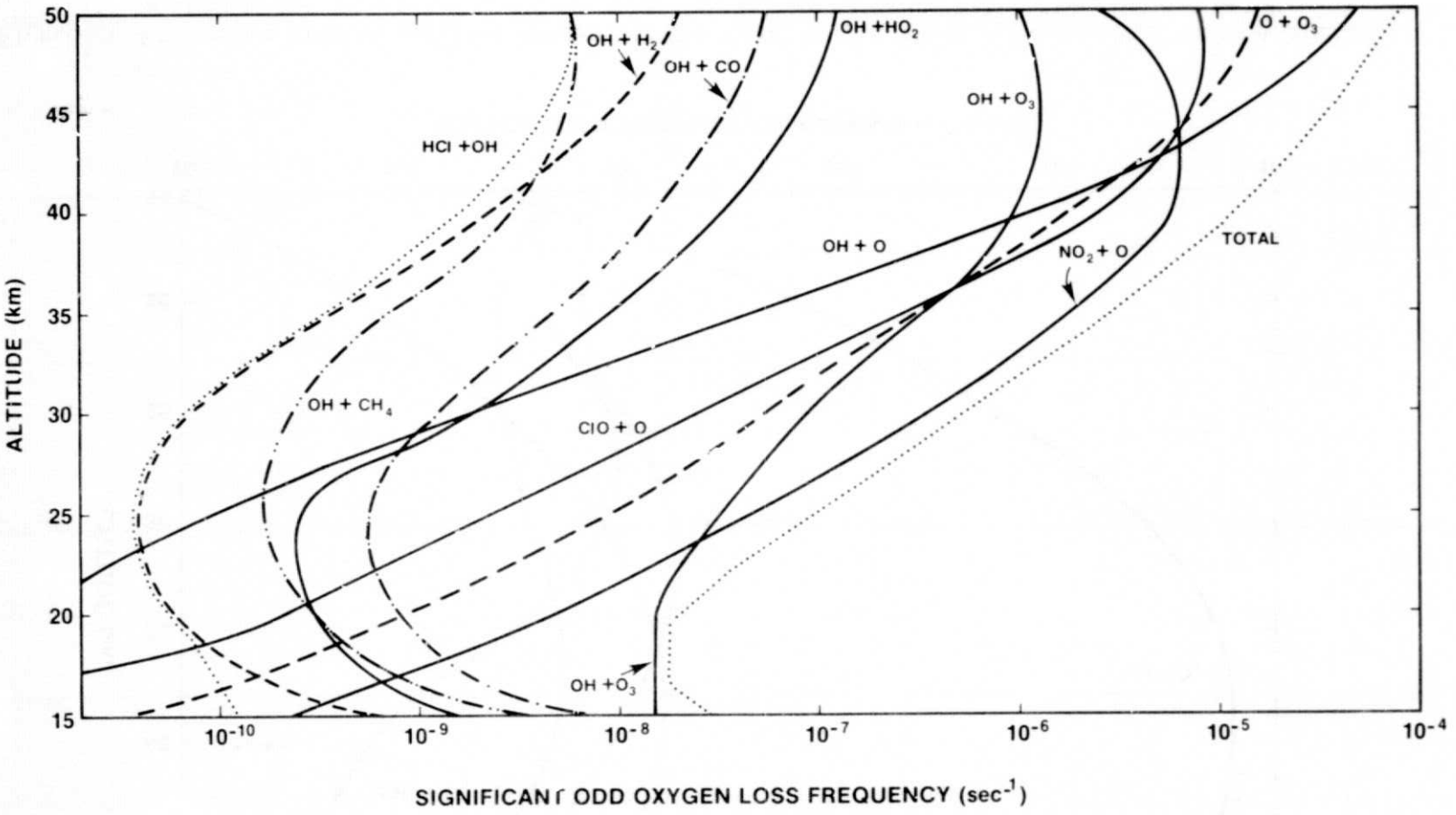
ALTITUDE (km)
50
45
40
35
30
25
20
15
HCl +OH
OH + H2
OH + CO
OH +HO2
OH + O3
O + O3
OH + O
NO2 + O
TOTAL
OH + CH4
ClO + O
OH +O3
10-10
10-9
10-8
10-7
10-6
10-5
10-4
SIGNIFICANT ODD OXYGEN LOSS FREQUENCY (sec-1)

Figure 2b.

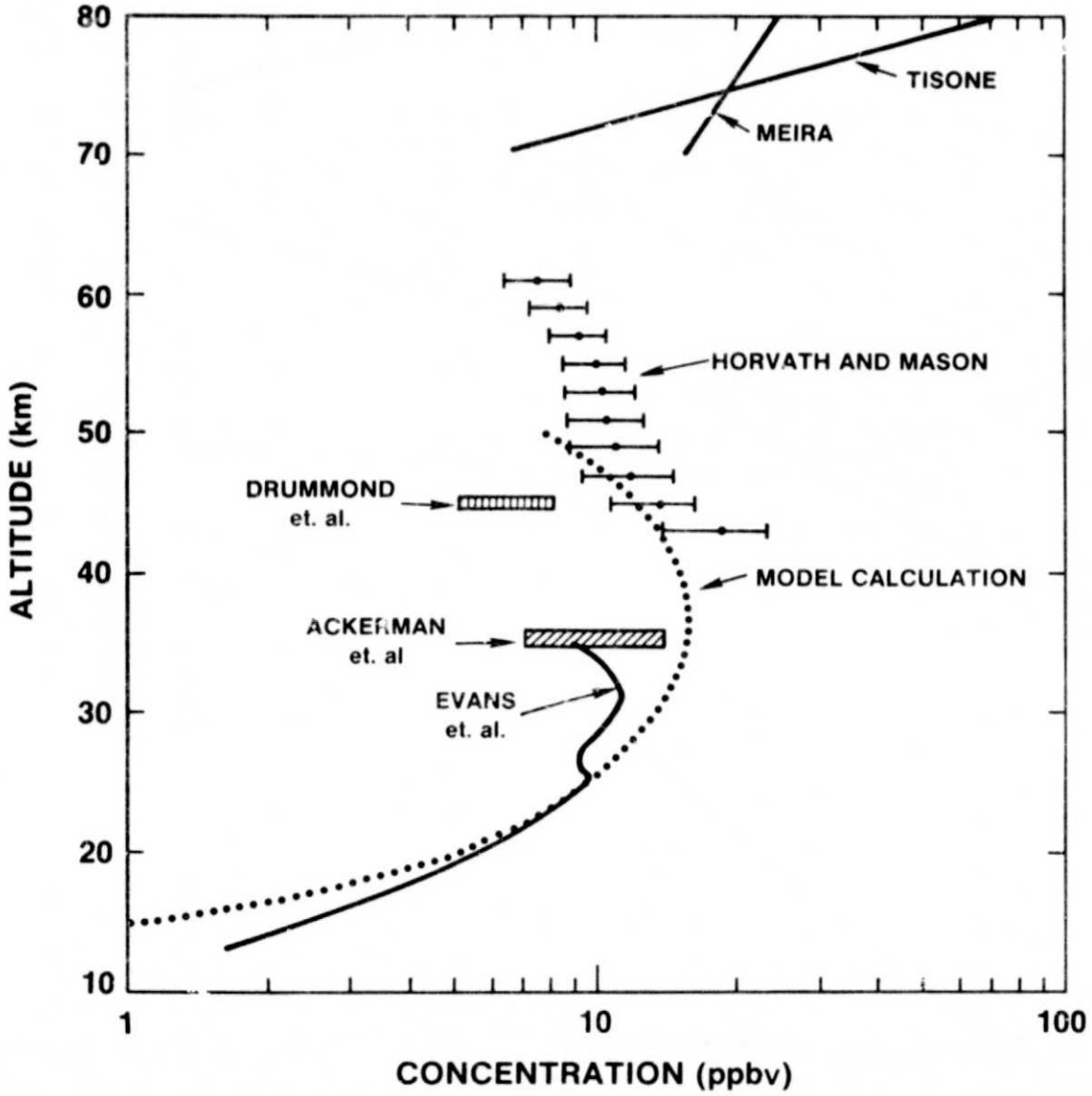

Figure 3. Measured data on total odd nitrogen content as a function of altitude and the calculated result assuming an upward flux of $5 \times 10^7 cm^{-2} sec^{-1}$ at 50 km.

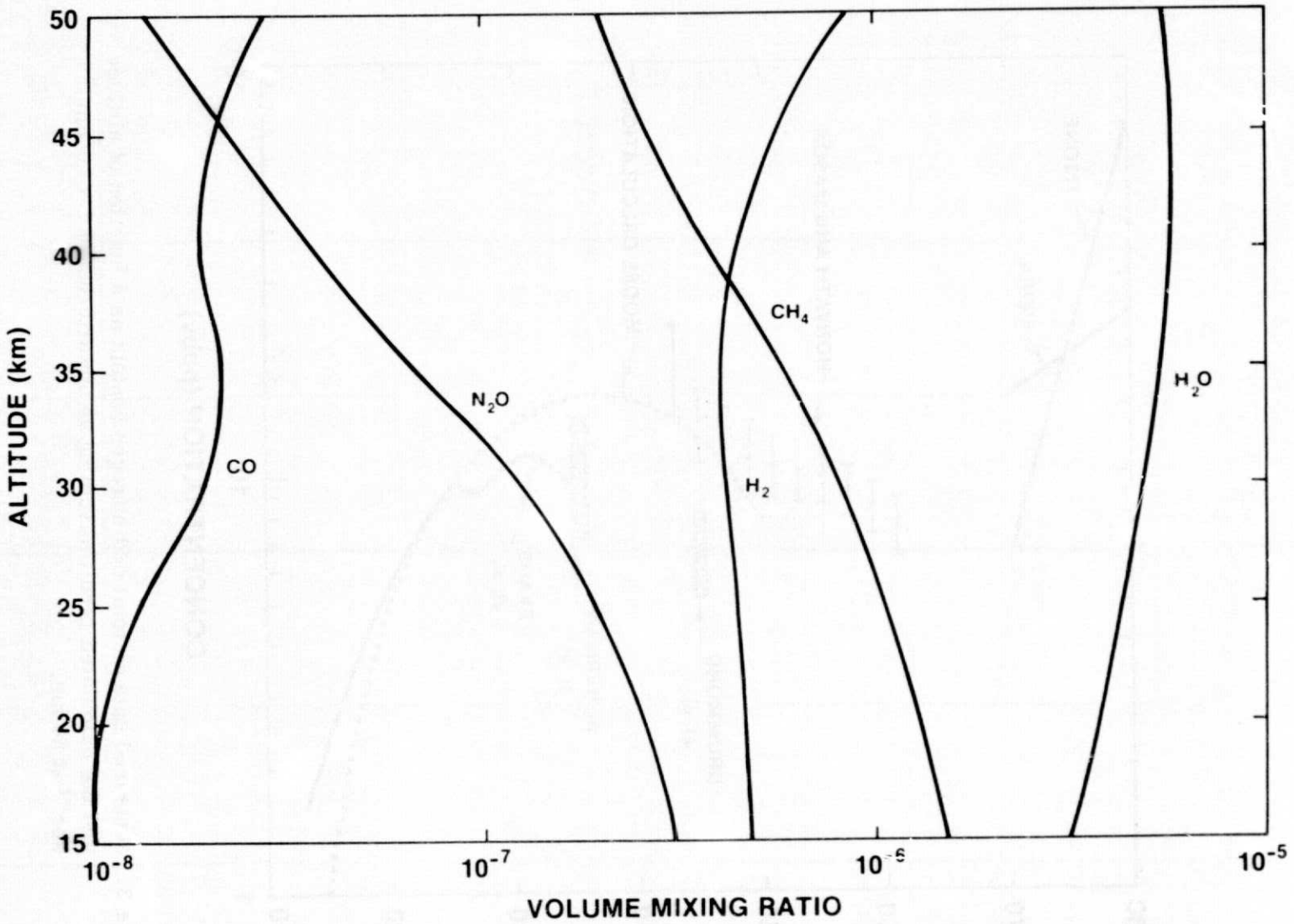

Figure 4. Mixing ratio profiles for CH_4, N_2O, CO, H_2 and H_2O.

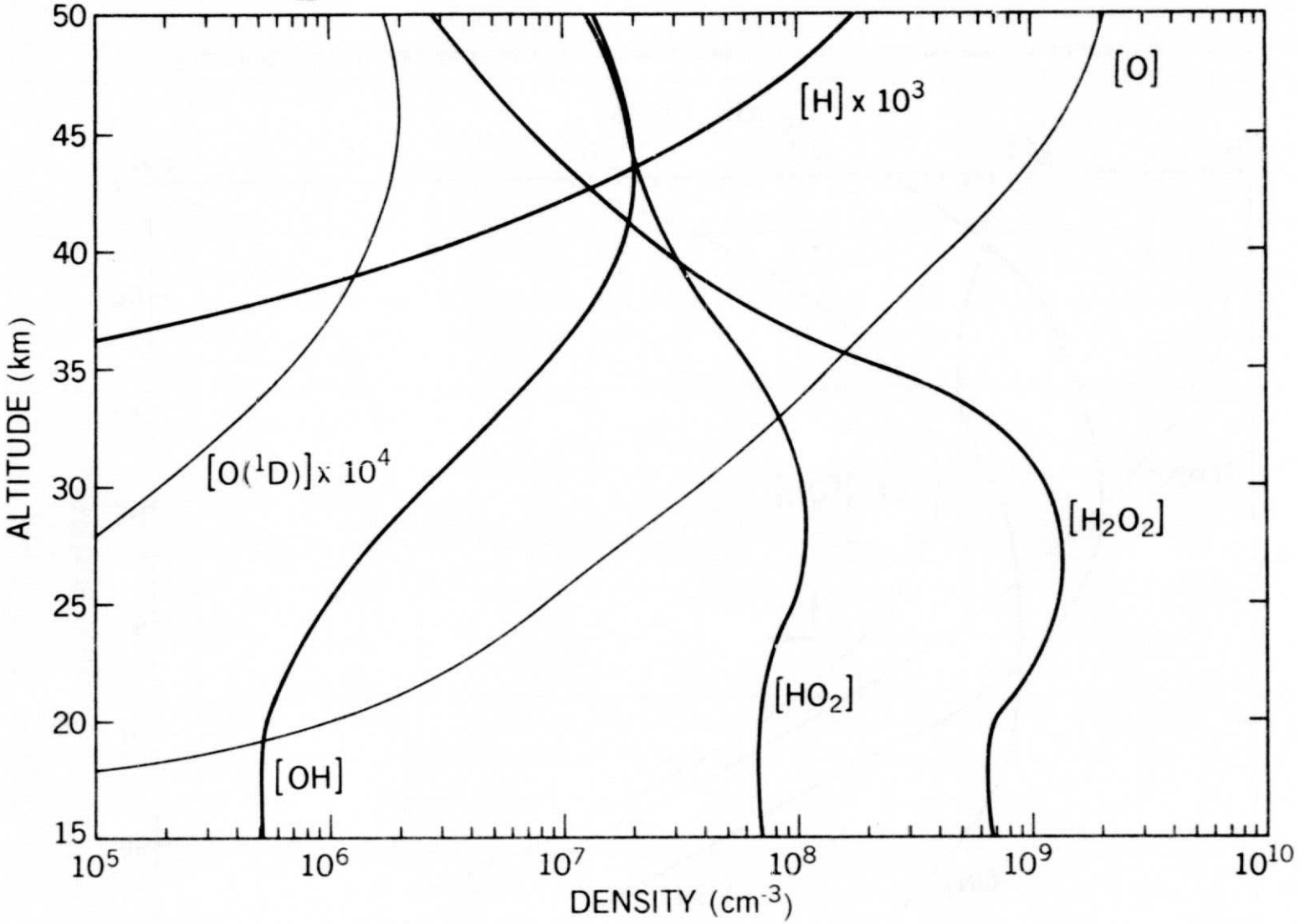

Figure 5. Calculated 24 hour average concentrations of HO_x constituents plus O and $O(^1D)$.

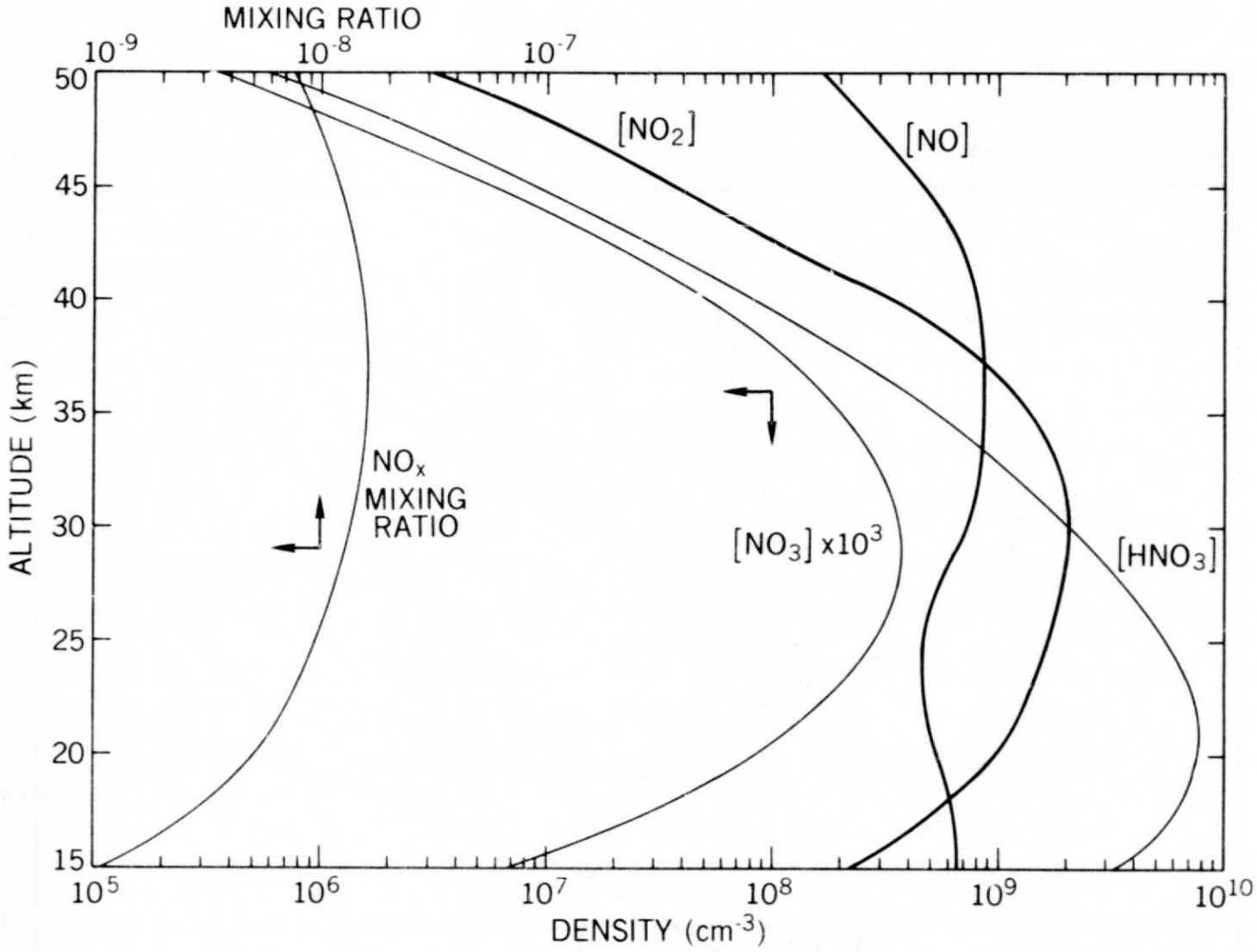

Figure 6. Calculated 24 hour average concentrations of odd nitrogen constituents.

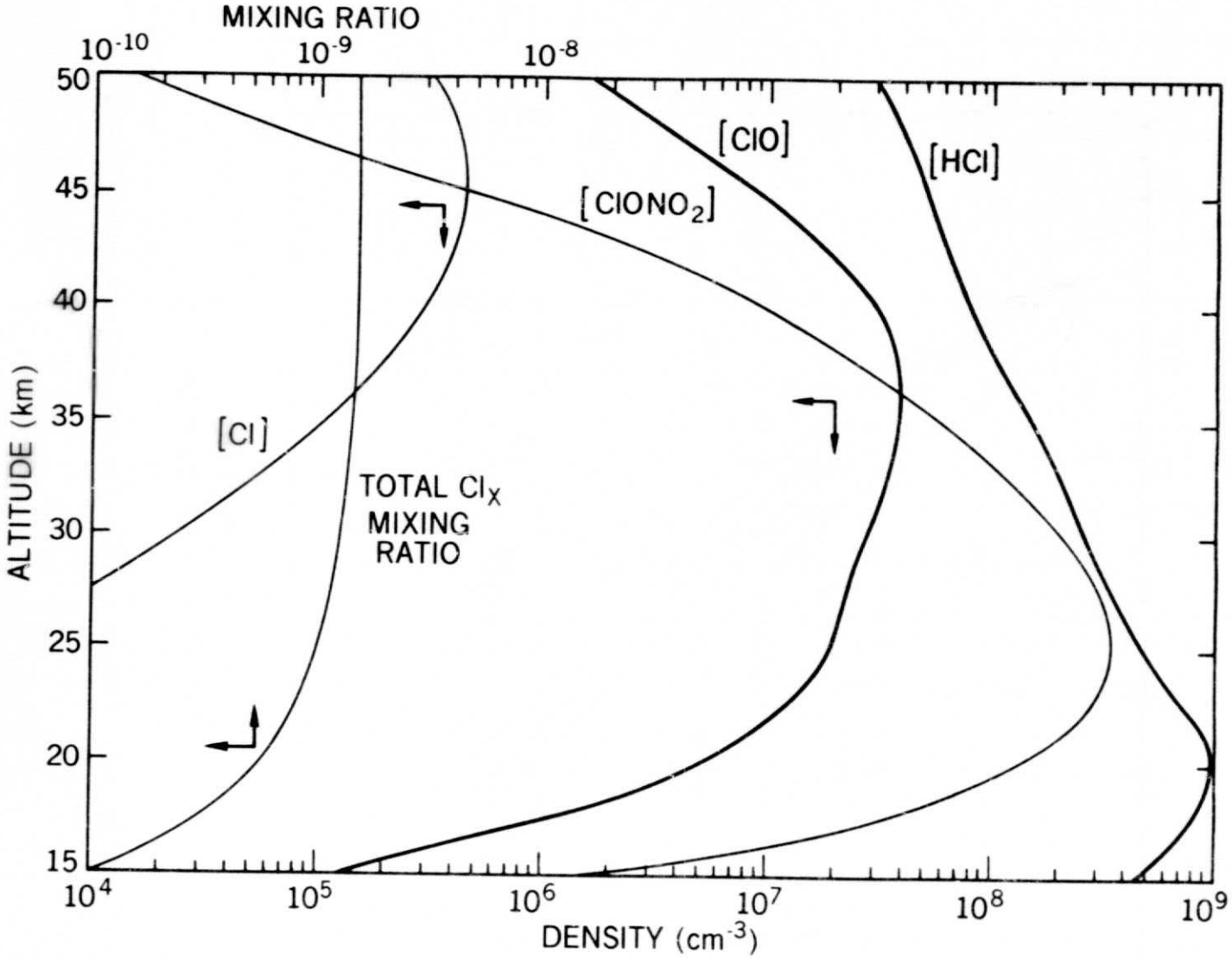

Figure 7. Calculated 24 hour average chlorine concentrations for an asymptotic mixing ratio of 1.5 ppbv ClX.

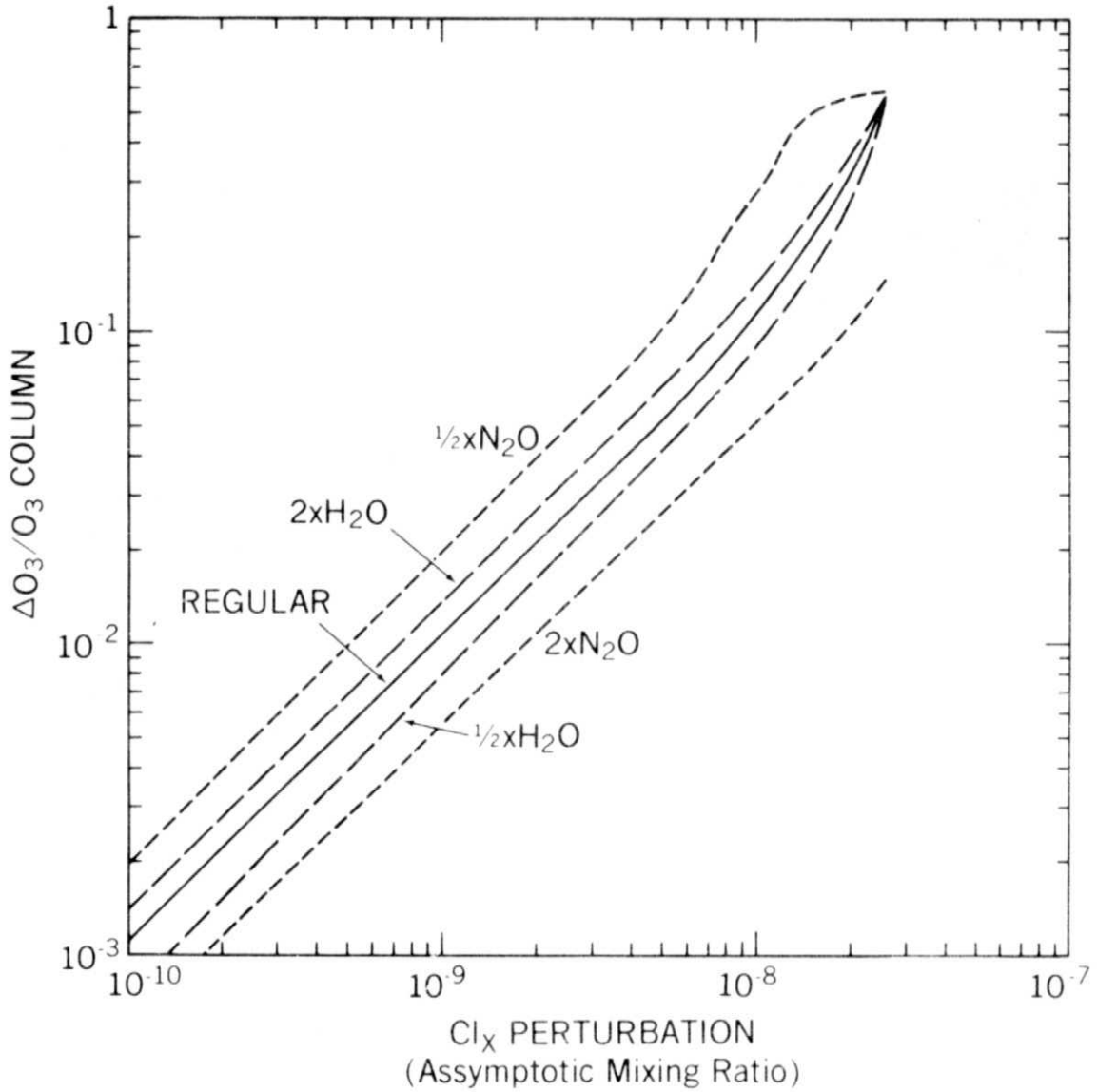

Figure 8. Fractional column ozone depletion as a function of asymptotic added Cl_X mixing ratio.

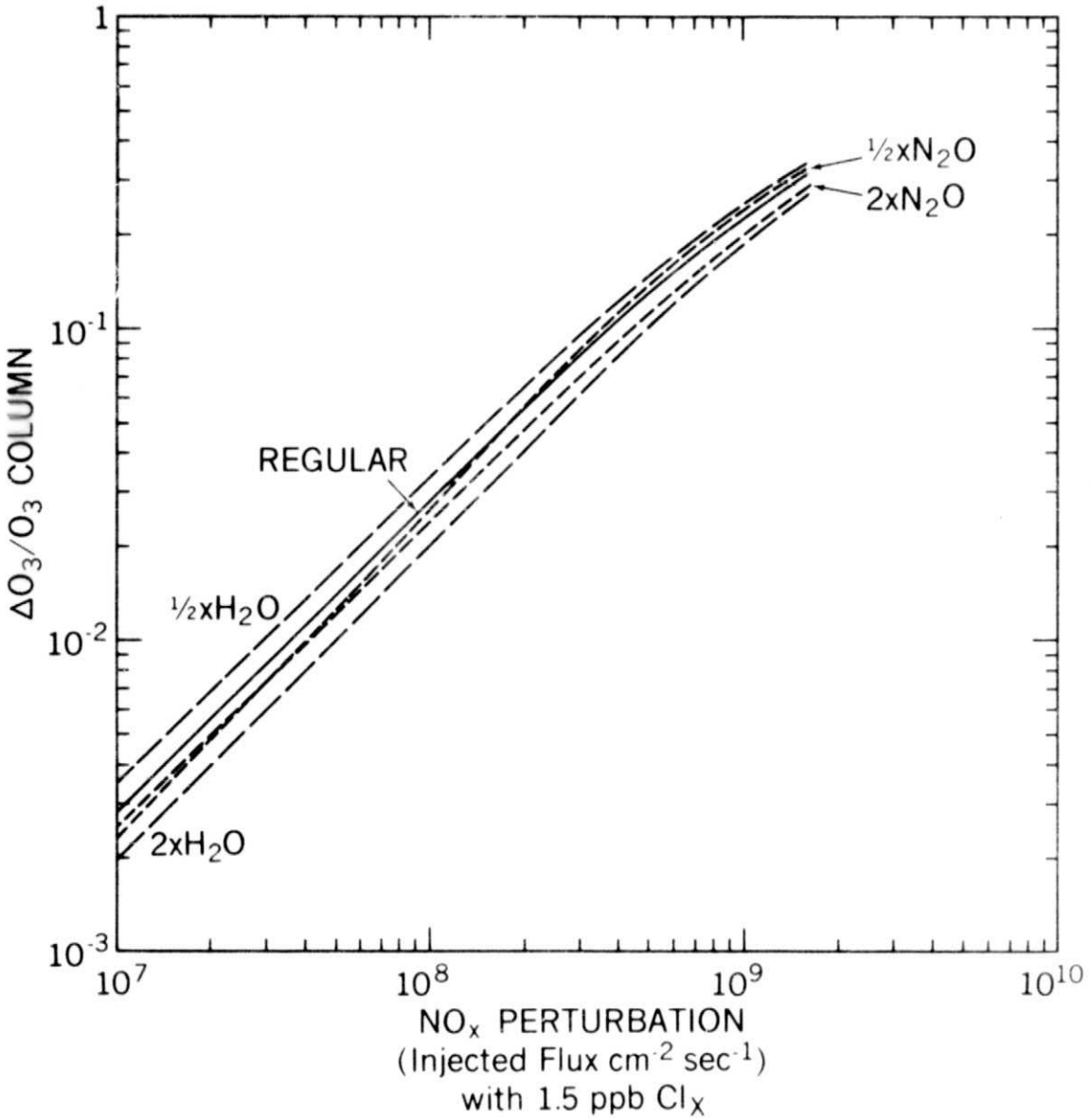

Figure 9. Fractional column ozone depletion as a function of added NO_x flux injected in a 5 km band about 20 km.